The Monte Carlo Method: Versatility Unbounded In A Dynamic Computing World
Chattanooga, Tennessee, April 17–21, 2005, on CD-ROM, American Nuclear Society, LaGrange Park, IL (2005)

APPLICATIONS OF THE MONTE CARLO ADJOINT SHIELDING METHODOLOGY

Roger A. Rydin and Craig R. Heimbach[1]
University of Virginia, Emeritus, Consultant U.S. Army
rarydin@earthlink.net

ABSTRACT

The Monte Carlo Adjoint Shielding (MASH) method has been developed to handle the case of a very complicated radiation shield that is irradiated from a distant source. It is not possible to accurately transport radiation to the vicinity of the shield and then through the shield to a dose point using Monte Carlo alone, even with bootstrap methods. Likewise, it is not possible to use discrete methods for the complete problem because of the shield geometry. The solution is to use a discrete method to transport radiation to the vicinity of the shield and then couple the incident radiation with an adjoint or importance Monte Carlo solution that starts all adjoint particles from the detector position. The methodology has been verified by experiment to give accuracies of 10 – 20% for shielded vehicles 200 – 1000 meters from a prompt fission source, and for vehicles situated on a large fallout field. The method has also been applied to a small concrete building and to a covered foxhole. Possible future applications are to large buildings in an urban environment, but more research has to be done to verify that the method is applicable to these problems.

Key Words: Monte Carlo, Adjoint, Discrete Ordinates, Vehicles, Buildings

1 INTRODUCTION

The calculation of the radiation fields inside closed structures, such as vehicles and buildings, is of considerable current interest. This is especially true when these shields are subjected to a mixed radiation field from a point source several kilometers away, or they are in the vicinity of a fallout field. Such problems bring the difficulties that the basic air-over-ground radiation field is not easy to calculate accurately at large distances, and then the shield may have a complex geometry that is also difficult to model. Deterministic methods that work well in transporting radiation from the source cannot handle the shield geometry. Stochastic methods that handle the shield geometry well cannot also accurately transport the radiation all the way from the source through the shield walls. The approach taken here is to use a combined methodology, where the radiation transport to the vicinity of the shield is done deterministically, and the transport to the dose point is done stochastically in the adjoint or importance mode. The two calculations are then coupled over a surrounding coupling surface to obtain the internal dose at a given dose position. The calculation has to be repeated for all dose points of interest.

The Monte Carlo Adjoint Shielding (MASH) code is based on the older Vehicle Code for Shielding (VCS) developed by Oak Ridge National Laboratory (ORNL) [1]. It consists of several separate pieces. The deterministic transport calculation is done by DORT (2D S_n) or TORT (3D S_n) with an un-collided flux correction. The adjoint Monte Carlo calculation is done by a modified version of the MORSE code. The dose for any given orientation of the shield is then evaluated with the DCR code, which couples the two together. The MASH code has been verified against experiment for a number of applications.

[1] formerly with Army Pulse Radiation Facility, now with NIST

2 THEORY

The DORT calculation gives the solution to the source problem,

$$Lf = S, \tag{1}$$

where L is the system description operator. The shield is considered to be a small perturbation, and is usually ignored, but a simplified shield can be put into the computation if the perturbation is not negligible, as was the case for a MASH medical therapy application [2]. The MORSE calculation is done in the adjoint mode, where only a small amount of external surrounding material, such as some air and ground, are included. The adjoint formulation is,

$$L^* f^* = R, \tag{2}$$

where R is the dose response function.

If we multiply Eq. 1 by f^*, multiply Eq. *2* by f, integrate over all space, energy and angle, and subtract the results, the terms involving L cancel and we obtain the result that,

$$\iint f^* S dV dP = \iint R f dV dP. \tag{3}$$

Here, P denotes energy-angle phase space. For a small "point" source and detector, the left-hand-side reduces to an integral over the source volume and the right-hand-side reduces to an integral over the detector volume, giving,

$$V_{source} \int_{source} f^* S dP = V_{\text{det}ector} \int_{\text{det}ector} R f dP = Dose. \tag{4}$$

Hence, in principle, the dose can be obtained by knowing the importance at the source or the flux at the detector. Since *neither* of these can be obtained accurately by a single computation, we compute the volume integral over a region containing the shield but not the source. A coupling surface is drawn around the shield, and the two calculations are combined in a surface integral,

$$Dose = \oiint_{couplingsurface} f^* f (\vec{\Omega} \bullet \vec{n}) dA dP, \tag{5}$$

where $\vec{\Omega} \bullet \vec{n}$ is the cosine of the angle between the particle direction and the inward normal to the surface.

3 DEFINITIONS

The Neutron Reduction Factor (NRF) at any internal location in the shield is defined as the neutron dose (in Gray) measured outside the shield divided by the neutron dose measured inside the shield. The Gamma Reduction Factor (GRF) is similarly defined for a gamma source.

These are the most easily measured quantities. The higher these values become, the better the shielding effect obtained.

However, the quantities that are usually desired are the protection factors. The Neutron Protection Factor (NPF) is defined as the ratio of the neutron dose measured outside the shield divided by the sum of the neutron dose and neutron-induced gamma dose measured inside the shield, which contains all the direct neutron effects. Likewise, the Gamma Protection Factor (GPF) is defined as the ratio of the gamma ray dose outside the shield divided by the gamma ray dose inside the shield that is directly attributable to the prompt gamma ray source. Because of these reallocations, the NPF is typically smaller than the NRF while the GPF is larger than the GRF.

In addition, we are interested in knowing the gamma ray Fallout Protection Factor (FPF), defined as the gamma dose measured outside the shield coming from a large uniform radioactive source deposited on the ground surrounding the shield to the dose measured at various locations inside the shield. The FPF is usually about twice as big as the GPF due to a greater attenuation in materials of the lower-energy fallout gamma rays.

4 APPLICATIONS

The MASH code has been experimentally verified at the Aberdeen Pulse Radiation Facility (APRF) for a number of box experiments [3,4]. Experimental data has been taken using tissue-equivalent ion chambers, Geiger-Mueller (GM) tubes, a four tube rotating gas-filled neutron spectrometer called ROSPEC, and a dose-integrating Sodium Iodide (NaI) gamma ray spectrometer called DOSPEC.

4.1 Fallout Field Tests

In 1996, two series of fallout radiation field tests were performed on a Russian T72 tank at the Etablissement Technique de Bourges (ETBS) in France [5,6]. The MASH model of the T72 consisted of over 10000 primitive bodies combined into more than 6000 material regions. Typically, 50000 starting particles were used for each case, giving an integral fractional standard deviation (FSD) of about 10%. Debugging of the geometrical model was done using the CGVIEW/ORGBUG graphics code developed by ORNL. A special 69-group cross-section library (DABL-69) was prepared by ORNL for this work.

4.1.1 Experimental details

In both tests, an 80-by-80-meter dirt field was sprayed with a liquid tagged with the fallout simulant La-140. One subset of measurements was made by driving the T72M1 into the middle of the field. For the first test only, a subsequent subset of measurements was made with the T72M1 positioned on one corner of the field in four separate 90 degree rotations, simulating the effect of the tank being in the middle of a 160-by-160-meter field. Both cases should approximately correspond to an infinite field.

For the first test, a second complete set of radiation measurements was made by spraying the La-140 fallout simulant over a 30-by-30-meter concrete pad. The T72M1 was driven to the center of the pad for the first measurement. The second subset of measurements was made with the tank positioned on one corner of the pad in four separate 90 degree rotations, simulating the effect of being in the middle of a 60-by-60-meter concrete pad. The smaller pad should act as if it were somewhat smaller than an infinite field. Since protection factors are ratios of measured or calculated values made at the same position, the effect of a finite field should be small, slightly overemphasizing the bottom of the tank relative to its sides.

Two types of radiation detectors were used in both tests. The first was a calibrated GM tube. The second was a NaI gamma ray spectrometer, configured to integrate the radiation dose over the measured spectrum (DOSPEC). The GM tube results in the first test, which were made using a portable Eberline detector, were not considered to be reliable because of detection system drift, which required frequent recalibration. The GM tube results were typically 10-20% lower than the DOSPEC results. Only a partial set of measurements was made with the GM tube. For the second test, a Phillips GM tube was used, which was cabled to remote power supplies and amplifiers to avoid the problems of the first test. Because of these limitations, only a few measurements were performed with the GM tube. Again, the protection factors measured with NaI were consistently higher than those measured with the GM detector. The difference is probably real, and is related to counting more low energy scattered gamma rays properly in terms of dose in the NaI spectrometer compared to counting them equally in the GM detector. Measurements were made at the seat position of the commander, gunner and driver, and head position of the commander and gunner.

4.1.2 Computational details

For a prompt source, the ground plane absorbs neutrons and creates a gamma ray source near the vehicle. Almost no neutrons or gamma rays penetrate the vehicle from below. To simulate this effect, the ground plane in the MASH model was taken to be 50 centimeters thick, which effectively shielded the bottom of the vehicle. The protection factor calculations done in this manner agreed quite well with measurements, thus validating the T72M1 model.

For fallout calculations, two modifications of the model were necessary. First, the ground was effectively removed from the tank model by making the ground very thin in order to allow coupling of all radiation entering from below the vehicle. Second, a large fallout field was used as the incident radiation source. This first source was modeled by Science Applications International Corporation (SAIC) for another purpose, so it used a U-235 fission product spectrum taken after 24 hours of decay.

The difference in protection factors calculated using a fission product spectrum and a La-140 spectrum should not be large. Protection factors are evaluated on a relative basis, and the gamma ray spectra are not greatly different for the two cases. When the computational model was placed anywhere inside of 50 meters from the boundary of the fission-product field, the FPF was independent of vehicle rotation, indicating that the field was effectively infinite. When the model was placed near the edge of the field, the differing shielding effectiveness of different sides of the vehicle was evident. All calculations were made near the center of the field.

A radiation field for La-140 was subsequently obtained from ORNL [7]. According to the ORNL report, the La-140 was distributed in the soil in a 0.3-cm-thick layer to account for penetration of the sprayed liquid into the soil.

4.1.3 Results

The experimental accuracy was estimated from the variance of the experimental data to be of the order of 10-15%. The computational accuracy was estimated from the FSD produced by MASH. Because there was a fairly strong variation in the experimental results as the vertical position of the detector was changed, several intermediate positions were calculated to explore the rate of change of these variations. The basic comparison between experiment and calculations is shown in table I for the first test series.

Table I. T72M1 La-140 Fallout Protection Factor Comparisons, Spring Test

POSITION	EXPT. NaI 30 by 30 m CONCRETE	EXPT. NaI 60 by 60 m CONCRETE	CALC. MASH Fission pr.	CALC. MASH La-140	EXPT. NaI 80 by 80 m DIRT	EXPT. NaI 160 by 160 m DIRT
C. SEAT	45.4 ± 7	58.6 ± 7	31.4 ± 3	36.1 ± 3	37.4 ± 7	31.3 ± 7
C. CHEST	----------	----------	34.5 ± 4	37.7 ± 4	----------	----------
C. NECK	----------	----------	45.7 ± 5	57.6 ± 5	----------	----------
C. HEAD	62.3 ± 10	60.6 ± 10	85.7 ± 8	62.7 ± 8	40.9 ± 10	26.7 ± 10
G. SEAT	41.7 ± 6	53.3 ± 6	38.6 ± 3	32.7 ± 3	39.3 ± 6	27.6 ± 6
G. CHEST	----------	----------	41.7 ± 5	50.2 ± 5	----------	----------
G. NECK	----------	----------	55.9 ± 6	50.1 ± 6	----------	----------
G. HEAD	62.4 ± 10	75.6 ± 10	73.8 ± 8	75.9 ± 8	47.6 ± 10	34.4 ± 10
D. SEAT	25.4 ± 3	19.3 ± 3	13.6 ± 1	14.6 ± 1	7.6 ± 3	10.9 ± 3
D. CHEST	----------	----------	16.6 ± 1	18.9 ± 1	----------	----------
VEHICLE AVERAGE	47.4	53.5	43.8	43.8	34.5	26.2

Several general observations can be made. First, the spread in the experimental data at the same experimental position for the various configurations is greater than 15%, indicating that some systematic differences exist between experiments. Second, the calculated results are in fairly good overall agreement with the experiments performed on the concrete pad. The calculated results are slightly lower, but tend to agree to the order of the combined error bars. Finally, the experimental data taken on the dirt field give significantly lower protection factors than are obtained on the concrete pad, and these results lie below the calculated results.

Somewhat more radioactive dirt would be thrown up into the air and deposited on the top of the vehicle from driving over the dirt field than from driving over the hard concrete pad, thus putting additional radiation sources on the vehicle that are not included in the calculations. These sources could lead to higher readings inside the vehicle and hence to lower apparent protection factors.

Nonetheless, the calculations are not in particularly bad agreement with the experiments done on the dirt field. The protection factor deviates the most on the low side for the driver, and this is entirely consistent with large amounts of dirt having been entrained on the tracks of the vehicle as it was driven across the dirt field, and remaining close to the driver during the measurements. The average fallout protection factor for the T72M1 can be safely taken to be 44 plus-or-minus 5, with the driver being considerably more vulnerable to fallout radiation than the other occupants of the vehicle. The final observation is that a strong local variation occurs in the calculated fallout protection factor close to the head, and may reflect strong local shielding in the vicinity of the turret. This makes the current experimental data difficult to interpret, because no effort was made to measure this effect. It is recommended that future experiments explore local variations in detector height at the crew positions more fully.

The corresponding results for protection factors computed with the ORNL La-140 source are also given in table I. The same general trends from head to gut are evident, although the results are somewhat different. Nevertheless, the averages for fission products and La-140 are about the same, and the experimental data are not sufficiently accurate to verify which of the results is more correct. It is unlikely that the hatch being open or closed has much to do with the results, unless contamination was tracked inside the vehicle during one of the measurements.

The experiments done on the T72M were considerably less extensive than those done on the T72M1, and emphasized the differences between protection factors for the hatch-open and hatch-closed cases. The results are shown in table II for the hatch-closed cases.

Table II. T72M La-140 Fallout Protection Factor Comparisons vs. La-140 Source, Fall Test

POSITION	CALC. MASH	CALC. MASH ORNL	EXPT. NaI 80 by 80 m DIRT	EXPT. GM 80 by 80 m DIRT
C. SEAT	36.1 ± 3	----------	----------	----------
C. CHEST	37.7 ± 4	----------	----------	----------
C. NECK	57.6 ± 5	----------	----------	----------
C. HEAD	62.7 ± 8	47.3	49.1 ± 10	35.5 ± 10
G. SEAT	32.7 ± 3	----------	----------	----------
G. CHEST	50.2 ± 5	----------	----------	----------
G. NECK	50.1 ± 6	----------	----------	----------
G. HEAD	75.9 ± 8	42.5	50.1 ± 10	42.8 ± 10
D. SEAT	14.6 ± 1	----------	----------	----------
D. CHEST	18.9 ± 1	----------	----------	22.7 ± 7
VEHICLE AVERAGE	43.8	----------	----------	----------

The small number of hatch-closed cases measured can be compared with the extensive calculations done here and the more limited number done at ORNL. The two calculated ORNL points are nominally in agreement with the fall 1996 experiment values, but these values are higher than those of the spring 1996 experiment by about 5-20%! Furthermore, since the

calculated results are very sensitive to the horizontal and vertical position of the source, and the presence or absence of the other crew members, it would not be difficult to account for the differences in the present and ORNL calculations by slight differences in source positioning or material mapping. Such differences cannot be resolved without more extensive experimental data and additional ORNL calculations.

4.2 Small Concrete Room

A more recent comparison was done at APRF on a small concrete room [9], to see if MASH would also work for hydrogen-containing shields with windows and doors. A rectangular concrete room, approximately 10 feet long by 6 feet wide by 6.5 feet high, containing only a single off-center 3 ft wide doorway, was built and tested at APRF for its shielding effectiveness against a mixed field of fast neutrons and gamma rays from the APRF reactor. This was the first test of a concrete structure typical of a moderately well shielded building. Of interest was the shielding effectiveness of such structures for both prompt neutron and gamma radiation from a point source and from a wide area radioactive fallout field such as might be created by a terrorist attack.

The analytical and experimental methods used for this type of radiation shielding problem have been well verified for relatively small, heavy, well-closed iron shields containing hydrocarbon-based radiation liners. It is now necessary to verify the ability of the same experimental and computational tools to treat very large structures containing typical building materials such as concrete, wood and glass. The first step in this verification consists of comparing dose rates at a number of different positions within a small concrete room that are expected to have significantly different shielding properties because of their locations relative to doors and windows.

In general, buildings are not nearly as good at shielding occupants from radiation, but they nevertheless provide a reasonable amount of protection. The amount of radiation protection depends on the distance above ground and the location in the room relative to the positions of doors and windows. To minimize exposure, it is best for the occupants to stay somewhere in the middle of the building and as far away as possible from direct sight of the radiation source coming through these openings.

4.2.1 Experimental details

The concrete room is a two-piece structure consisting of a bottom half and a top half that fit together using a V-groove technique to avoid radiation streaming through the cracks [8]. In addition to the basic room, an extra self-standing L-shaped pedestal and wall were cast that allowed doubling of the 6 inch thickness of one of the side walls when it was leaned against the room. A photograph of the room with the extra sidewall in place is shown in figure 1. The room was positioned 400 meters from the reactor, which acted like a point source of radiation 14 meters above the ground.

Neutron spectrometers (ROSPEC) and gamma ray dosimeters (DOSPEC) were placed inside the room a meter above the floor at three basic locations: A) directly in front of the door; B) in the middle of the room; and C) far into the room. These variations

emphasize the increasing shadow-shielding effect of the walls. A few special detector locations were added to check local radiation field gradients. Measurements were made with the door facing the reactor, and with the room rotated clockwise by 90, 180, and 270 degrees, which forces the radiation to scatter before it can enter the opening. The detectors were also placed one meter above the ground in the open, well away from the room, to obtain the free-in-air comparison doses that would be received in the absence of the shield.

Figure 1. Photograph of the Concrete Room Radiation Shield with Extra Side Wall.

4.2.2 Results

The experimental and computed NRF results for the concrete room without the extra wall are given in table III. In general, the agreement between calculation and experiment is of the order of 5 to 10% for all positions. There is considerably less protection when the radiation can directly enter the door (0 degrees), and the protection increases when the detector is moved further away from the door, from A to B and then to C, giving additional shadow shielding from the direct source. The same general trends are observed for the NRF with the extra wall in place, but the protection factors are slightly higher corresponding to the presence of the extra absorber. The protection factors are highest for the case where the radiation has to pass directly through the extra wall (270 degrees). Given the excellent agreement between calculated and experimental NRF values, the corresponding calculated NPF factors become meaningful. It can readily be seen that the NPF is approximately 2/3 of the NRF.

The experimental and computed GRF results for the concrete room without the extra wall are given in table IV. In general, the agreement between calculation and experiment is of the order of 15 to 25% for all positions. There is considerably less protection when the radiation can directly enter the door (0 degrees), and the protection increases when the detector is moved further away from the door giving additional shadow shielding.

Table III. Experimental and Calculated NRF and NPF for the Concrete Room, No Extra Wall

Detector	Type	Angle 0	Angle 90	Angle 180	Angle 270	Average
A (door)	NRF Expt.	1.66	5.75	4.69	4.00	4.03
	NRF Comp.	2.18	5.21	4.65	4.09	4.17
	NPF	1.70	3.18	2.95	2.68	2.71
B (center)	NRF Expt.	3.66	5.23	5.00	5.08	4.74
	NRF Comp.	3.41	5.22	4.62	5.02	4.44
	NPF	2.32	3.13	2.90	3.03	2.79
C (right)	NRF Expt.	4.98	4.52	5.03	6.14	5.17
	NRF Comp.	4.51	4.46	4.90	5.68	4.73
	NPF	2.82	2.80	2.97	3.32	2.91

For gamma rays, the calculated reduction factors are all higher than the experimental values. For the case of the detector in the doorway directly facing the source, the experimental value is *less than unity*, indicating that neutrons captured in the back wall actually produce *more* detected gamma dose than is shielded out by the rest of the shield. These low energy gamma rays are apparently not included accurately in the calculations. This is probably due to the discrete energy group structure used in MASH, which doesn't have enough detail in this energy region. The group structure was originally chosen for the analysis of well-shielded vehicles without direct openings. Nevertheless, since all of the GRF values are near unity, the agreement is actually quite good.

Table IV. Experimental and Calculated GRF, GPF and FPF for the Concrete Room, No Extra Wall

Detector	Type	Angle 0	Angle 90	Angle 180	Angle 270	Average
A (door)	GRF Expt.	0.88	1.17	1.10	1.05	1.05
	GRF Comp.	1.02	1.37	1.33	1.28	1.28
	GPF	2.07	3.86	3.57	3.50	3.43
	FPF	7.08	7.08	7.08	7.08	7.08
B (center)	GRF Expt.	1.05	1.15	1.15	1.09	1.11
	GRF Comp.	1.19	1.33	1.31	1.31	1.28
	GPF	3.14	3.81	3.64	3.79	3.61
	FPF	8.65	8.65	8.65	8.65	8.65
C (right)	GRF Expt.	1.06	1.10	1.08	1.12	1.09
	GRF Comp.	1.30	1.29	1.31	1.39	1.32
	GPF	3.91	3.72	3.92	4.18	3.94
	FPF	12.2	12.2	12.2	12.2	12.2

For the case with the added wall, all of the trends of the previous case are repeated, but the GRF values are slightly higher. The highest reduction occurs for the case where the radiation passes directly through the extra wall (270 degrees).

Given the excellent agreement between calculated and experimental GRF values, the corresponding calculated GPF factors become meaningful. These comparisons are also given in

table IV, along with the calculated fallout FPF values. It can readily be seen that the GPF is more than double the GRF when the neutron contribution to gamma dose is removed. Furthermore, the FPF is more than double the GPF due to the lower energy and different directionality of the source. There is no rotational effect for the FPF, since the room is surrounded by the source.

4.3 Foxhole

It is of interest to know the relative radiation protection offered to a person inside a foxhole compared to standing out in the open. For this purpose, a crude Combinatorial Geometry model of a foxhole was constructed using the MASH formalism. The hole was 1.64 meters wide, by 0.82 meters long by 1.35 meters deep. It was equipped with a berm in front, a partial top cover consisting of a wooden support and a dirt cover, and a berm in back with a centered access hole. One person stands in the front-center position in the hole, while the second one stands at the front-side position. The calculations include the shielding offered by the other person's presence.

The computational results are given in table V. It can easily be seen that the most radiation strikes the head, which is only partially protected by the berm and top cover. As the depth increases, considerably more protection is offered to the chest and gut by the sides of the foxhole. It is also apparent that dirt is a better neutron shield than it is a gamma shield.

Table V. Calculated Foxhole Protection Factors

Position	NPF	GPF	FPF
Center Head	3.09	1.95	12.73
Center Chest	4.29	2.92	27.27
Center Gut	6.60	4.41	44.83
Side Head	2.72	1.77	8.05
Side Chest	4.65	2.83	29.68
Side Gut	8.57	4.68	64.32
Average	5.0	3.1	31.

For the prompt source, the gamma field is distributed above the foxhole by scattering. It is clear that most of the radiation enters the foxhole from above, which is why there is so little difference between the two calculated positions. It is probably more accurate to take the protection factors at the head positions as defining the risk to the person, than using the average values. Hence, NPF ~ 2.9, and GPF ~ 1.9.

For the fallout scenario, the protection factor is much higher than for a prompt source. The reason is that the radiation field is concentrated along the ground, and there is not much downward scattered radiation present from above the foxhole. Hence, most of the gamma radiation must penetrate the dirt in order to reach the occupant. What little radiation that has scattered above the foxhole is degraded in energy, which means that it is easier to shield and it deposits less relative dose per event. The net result is that the effective FPF ~ 10, or about 5 times the GPF!

4.4 Large Buildings

Future computations will be made for more complicated situations, such as a building surrounded by other buildings in an urban environment. To facilitate model building, a fortran90 code was written that allows several MASH models to be replicated, rotated and stacked to automatically create a new MASH model. An example is shown below.

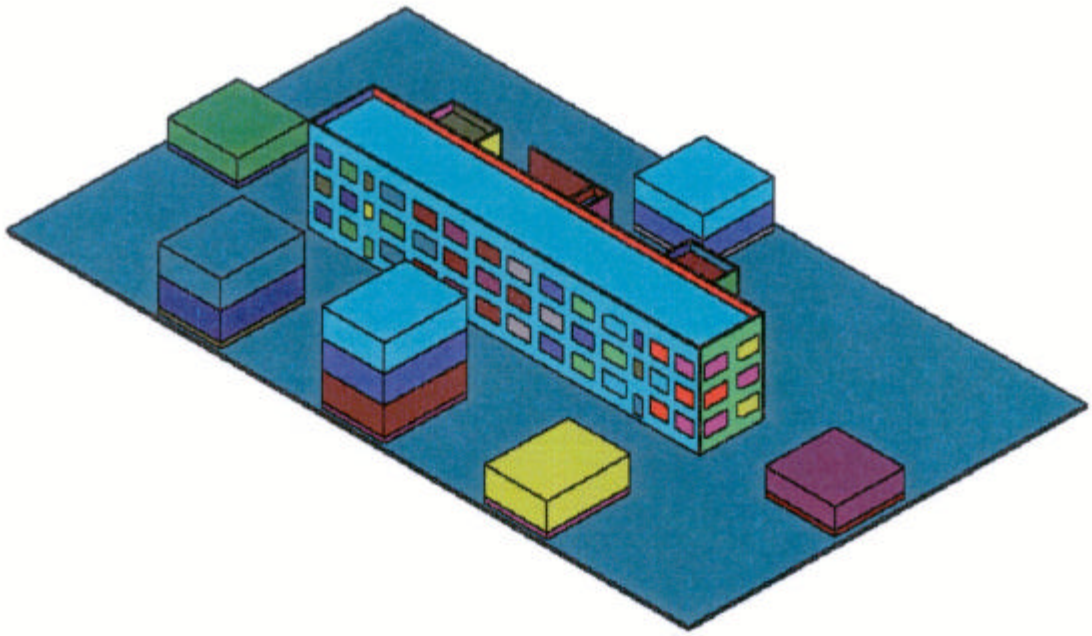

Figure 2. Schoolhouse Surrounded by Small Buildings

Even though such a model can be constructed, it is not yet known what is the effect on accuracy of using a very large MASH coupling volume. A preliminary evaluation of some large building structures also indicates that MASH may not be practical for this application because of the long running time per case and the large number of internal points that would have to be calculated to obtain meaningful average shielding values on different floors of a building. .

The TORT code was initially assumed to be the method of choice for large geometrically regular structures like tall buildings because it evaluates all points simultaneously and can give direct averages over floors. However, TORT has some physical limitations when applied to structures like a 10-story building. Specifically, due to memory and running time limitations, numerical instabilities and iterative convergence problems have arisen. It is not clear that these problems can be resolved with the current generation of computers. Furthermore, there is a question of how to include the very large ground plane source needed to reach an equilibrium dose field.

The ORNL QAD point-kernel code uses a MASH model, and appears to be an excellent fast running replacement for TORT when only radioactive dispersions are considered. However, the point buildup-factor corrections used in the code to correct the dose rates at each floor have never been validated for very large and/or tall buildings.

5 CONCLUSIONS

The MASH methodology has been successfully applied to a number of small but complicated shields placed more than 400 meters from a prompt fission radiation source or placed on an extensive fallout field. Only further research will allow extension of these methods to very large structures in urban environments, for which neither experimental data nor computations are available.

6 REFERENCES

1. W. A. Rhodes, "Development of a Code System for Determining Radiation Protection of Armored Vehicles," ORNL-TM-4664 (1974).
2. T. R. Hubbard and R. A. Rydin, "Treatment Room Dose Determinations Using the Monte Carlo Adjoint Shielding (MASH) Code," *Eighth International Symposium on Neutron Capture Therapy for Cancer*, San Diego, CA, 1998.
3. R. A. Rydin, C. R. Heimbach and H. Caton, "The Effects of Holes and Gaps on the Shielding Effectiveness of a Lined Steel Box," *Topical Meeting on Advances in Nuclear Engineering Computation and Radiation Shielding*, Santa Fe, NM, 1989.
4. J. O. Johnson, J. D. Drischler and J. M. Barnes, "Analysis of the Fall-1989 Two Meter Box Test Bed Experiments Performed at the Army Pulse Radiation Facility (APRF)," ORNL-TM-11777, May 1991.
5. C. R. Heimbach, M. A. Oliver and M. B. Stanka, "Research Report of the Radiation Fallout Tests at Etablissement Technique de Bourges", Report No. ATC8071 (limited distribution), U. S. Army Aberdeen Test Center, April 1998.
6. C. R. Heimbach, M. A. Oliver, M. B. Stanka, "Research Report of the Radiation Fallout Tests at Etablissement Technique de Bourges, Fall 1996", REPORT NO. ATC-8103 (limited distribution), U. S. Army Aberdeen Test Center, September 1998.
7. J. M. Barnes, R. T. Santoro, "Analysis of the Radiation Fallout Tests at ETBS, France (Fall 1996), ORNL/TM-2000/1, January 2000.
8. C. R. Heimbach, "Radiation Protection of a Concrete Bunker", REPORT NO. ATC-8378 (limited distribution), U. S. Army Aberdeen Test Center, June 2001.